Heliyon 9 (2023) e17658

Contents lists available at ScienceDirect

Heliyon

journal homepage: www.cell.com/heliyon

Numerical investigation of MHD flow of hyperbolic tangent nanofluid over a non-linear stretching sheet

Iftikhar Ahmed [a], Metib Alghamdi [b], Muhammad Amjad [a,*], Faisal Aziz [a], Tanvir Akbar [a], Taseer Muhammad [b]

[a] Department of Mathematics, COMSATS University Islamabad, Islamabad Campus, 45550, Pakistan
[b] Department of Mathematics, College of Sciences, King Khalid University, Abha, 61413, Saudi Arabia

ARTICLE INFO

Keywords:
Hyperbolic tangent
MHD
Non-linear stretching
Nanofluids
bvp4c

ABSTRACT

This research investigates two-dimensional MHD incompressible boundary layer Hyperbolic Tangent nanofluid flow across a non-linear stretching plate. Similarity transformations are employed to convert the governing non-linear partial differential equations (PDEs) into coupled non-linear ordinary differential equations (ODEs). The MATLAB built-in routine bvp4c has been used for finding the numerical solutions of the dimensionless velocity, temperature, and concentration profiles. The current findings are validated with already published results. The influence of some important parameters on the velocity, temperature, and concentration profiles are displayed through graphs and tables. It is observed that for increasing values of magnetic parameter M and hyperbolic Tangent parameter We, the boundary layer thickness of the velocity profile decreases while it increases for the temperature profile.

1. Introduction

The analysis of non-Newtonian fluids has been one of the most significant advances in the previous two decades. As a result, research into the thermophysical characteristics of these fluids has sparked a lot of interest. Due to their widespread industrial and technological uses, there is a wealth of literature on this issue, including analytic and numerical solutions. In the category of non-Newtonian fluid models, the tangent hyperbolic fluid (THF) model is one of the most important. According to laboratory experiments, this model well describes the shear thinning phenomenon. This model also properly illustrated blood flow. The THF model is used in chemical engineering systems that offer several benefits over other non-Newtonian fluid models. Blood, paint, whipped cream, ketchup, nail polish, and such kind of other THF are common examples. Shahzad et al. [1] examined a 2D tangent hyperbolic nanofluid passing across a continuous surface recently. The impact of heat transmission on the magnetized flow of THF through a stretchable sheet was examined by Zakir et al. [2]. Akbar et al. [3] explored the MHD boundary layer flow of THF models numerically. Ibrahim [4] discussed the impacts of thermal radiation on magnetized THF with nanoparticles passing through an expanding sheet with convective boundary conditions (BCs) and 2nd order slip.

Magnetohydrodynamics (MHD) flows are significant both theoretically and practically. In the fluid dynamics, MHD shows a significant role. MHD is the investigation of the flow of an electrically conducting fluid in the presence of a magnetic field. MHD concepts are used in a variety of technological fields, including the oil industry, crude oil purification, molten metal refining, and so on. In the

* Corresponding author.
E-mail address: muhammadamjad2955@gmail.com (M. Amjad).

https://doi.org/10.1016/j.heliyon.2023.e17658
Received 13 February 2023; Received in revised form 26 May 2023; Accepted 25 June 2023
Available online 26 June 2023

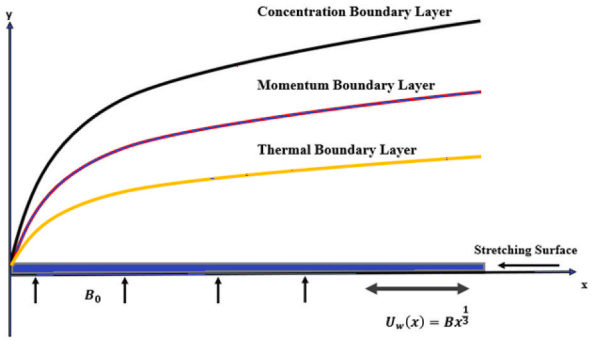

Fig. 1. Schematic flow diagram.

fields of glass fibre manufacture, metallurgy, and polymer technology. Andersson et al. [5] investigated heat transmission in a flow of MHD visco-elastic liquid through a continuous stretching surface. Kameswaran et al. [6] studied the impact of linear velocity on the stretching/shrinking wall, considering hydromagnetic, and viscous dissipation, chemical reaction. Chakrabarti et al. [7] investigated the heat transfer analysis of viscous fluid flow wit MHD and estimated the boundary layer solution. Hussain et al. [8] investigated the thermophysical properties of THF flow within a non-linear stretching plate with convective boundary conditions (CBCs), and viscous dissipation. Malik et al. [9] examined the MHD flow of THF model across a stretching cylinder numerically. Other research on MHD fluxes include [10–19].

In fluid mechanics, stretching plate play an important role, because of their wide range of applications and its usage in evaluating fluid behavior in boundary-driven flows For Newtonian and non-Newtonian fluids, different geometries and stretching velocities have been investigated. Imran Ullah et al. [20] investigated the magnetized Casson fluid flow through a non-linear stretched porous plate with slip boundary condition. Hayat et al. [21] examine MHD convective nano-fluid flow with varying thickness across a non-linear stretched sheet. Kameswaran et al. [22] examined the impact of thermophoretic and non-linear convection. Cortell [23] addressed the radiative effect and heat transport fluid through a non-linear stretched sheet.

A nanofluid is the combination of the base fluid, such as water [24], with nanometer-sized particles. It is commonly assumed that nanoparticles improve the heat transfer performance of nanofluids. Choi [25] proposed the idea of nanofluids in 1995 to improve heat transfer rates. Gharami et al. [26] studied the MHD influence on an unstable stream of tangent hyperbolic nanofluid passing over an effective chemical development. Aslani et al. [27] studied the MHD consequences and Poiseuille micropolar flow stability analysis. Gkountas et al. [28] inspected the influence of the heat transfer applying Al2O3 and water nanofluid. The most recent study has been summarized on nanofluid can be shown [29–36].

In this paper, governing equations are nonlinear PDEs, which will be transformed into high nonlinear ODEs by adopting suitable similarity transformations and then MATLAB solver bvp4c will be used to solve system of ODEs. Tables and graphs are used to evaluate the impact of including physical characteristics. To the best of the author's knowledge, no one has investigated this issue. We hope that the viscous dissipation this work will be valuable in better understanding and researching expanding developments in an industrialized context.

2. Problem description

The 2D incompressible boundary layer fluid flow is assumed over a non-linear stretching plate. The fluid is Tangent Hyperbolic and MHD effects are also considered. We have assumed that the plate is stretching with variable velocity $u = U_w = Bx^{\frac{1}{3}}$ along the x-axis, and the y-direction is perpendicular to the x -direction. The flow is exposed to a transverse magnetic field $B^* = \frac{B_0}{x^{\frac{1}{3}}}$ in a vertical direction. In addition, C, T, The T_w, C_w, T_∞ and C_∞ stand for the concentration profile, temperature profile, wall temperature, wall concentration, ambient temperature, and ambient concentration respectively. The under-discussion model [19,37,38] is illustrated in Fig. 1

The Governing equations [37,39,40] are:

$$\frac{\partial u}{\partial x}+\frac{\partial v}{\partial y}=0, \tag{1}$$

$$u\frac{\partial u}{\partial x}+v\frac{\partial u}{\partial y}=\nu\left((1-n)+\sqrt{2}n\Gamma\frac{\partial u}{\partial y}\right)\frac{\partial^2 u}{\partial y^2}-\frac{\sigma B_0^2}{\rho_f}u, \tag{2}$$

$$u\frac{\partial T}{\partial x}+v\frac{\partial T}{\partial y}=\alpha\frac{\partial^2 T}{\partial y^2}+\frac{\rho_p c_p}{\rho c}\left[D_B\frac{\partial C}{\partial y}\frac{\partial T}{\partial y}+\frac{D_T}{T_\infty}\left(\frac{\partial T}{\partial y}\right)^2\right], \tag{3}$$

$$u\frac{\partial C}{\partial x}+v\frac{\partial C}{\partial y}=\frac{D_T}{T_\infty}\frac{\partial^2 T}{\partial y^2}+D_B\frac{\partial^2 C}{\partial y^2}. \tag{4}$$

Table 1
Effect of skin friction coefficient $Re_x c_f$ on n, We, and M.

n	We	M	$-\left((1-n)+\frac{n}{2}We f''(0)\right)f''(0)$
0.1	0.5	0.5	0.932163
0.2			1.016640
0.3			1.096308
0.3	0.1		0.808646
	0.2		0.800995
	0.3		0.793042
		0.1	0.600077
		0.2	0.648990
		0.3	0.694237

Table 2
Effect of $-\theta'(0)$ and $-g'(0)$ on n, We, M, Pr, Le, Nc, Nbt, and Sc.

n	We	M	Pr	Le	Nc	Nbt	Sc	$-\theta'(0)$	$-g'(0)$
0.1	0.5	0.5	0.5	3.0	0.5	2.0	2.0	0.209793	0.627703
0.2								0.200519	0.610165
0.3								0.189534	0.587607
0.3	0.1							0.191385	0.597856
	0.2							0.190240	0.595289
	0.3							0.189048	0.592585
		0.1						0.218816	0.645472
		0.2						0.209244	0.629025
		0.3						0.200779	0.613862
			0.1					0.063744	0.635271
			0.2					0.091398	0.622241
			0.3					0.122145	0.609816
			0.5	0.1				0.001045	0.651501
				0.2				0.016199	0.646421
				0.3				0.039595	0.639343
					0.1			0.212768	0.576634
					0.2			0.205897	0.579276
					0.3			0.199232	0.581832
						0.1		0.104454	0.046621
						0.2		0.139576	0.224951
						0.3		0.154879	0.330159
							0.1	0.206840	−0.005330
							0.2	0.204218	0.026183
							0.3	0.201683	0.062341

Table 3
Comparison table of $-\theta'(0)$ for We and Pr.

We	Pr	Kamran et al. [37]	Present
0.0		0.319	0.319
0.2		0.318	0.318
0.4		0.317	0.317
	0.2	0.231	0.231
	0.6	0.347	0.348
	1.2	0.521	0.521

here u, v, ϑ, σ, B_0, Γ, c, ρ, D_B, α, and T_∞ represents the longitudinal and normal velocity components, kinematic viscosity, electrical conductivity, magnetic field, time constant, specific heat, density, Brownian diffusivity, thermal conductivity, and ambient temperature respectively.

The BCs that are taken into consideration are as follows:

$$u = U_w = Bx^{\frac{1}{3}},\ v = 0,\ T = T_w,\ C = C_w \text{ at } y = 0.$$

$$u \to 0, T \to 0, C \to 0 \text{ as } y \to \infty \tag{5}$$

To solve the governing equations (2)–(4), the following similarity transformation is performed.

$$u = Bx^{\frac{1}{3}} f'(\eta), v = -\frac{\sqrt{\nu B}}{3x^{\frac{1}{3}}}(2f(\eta) - \eta f'(\eta))$$

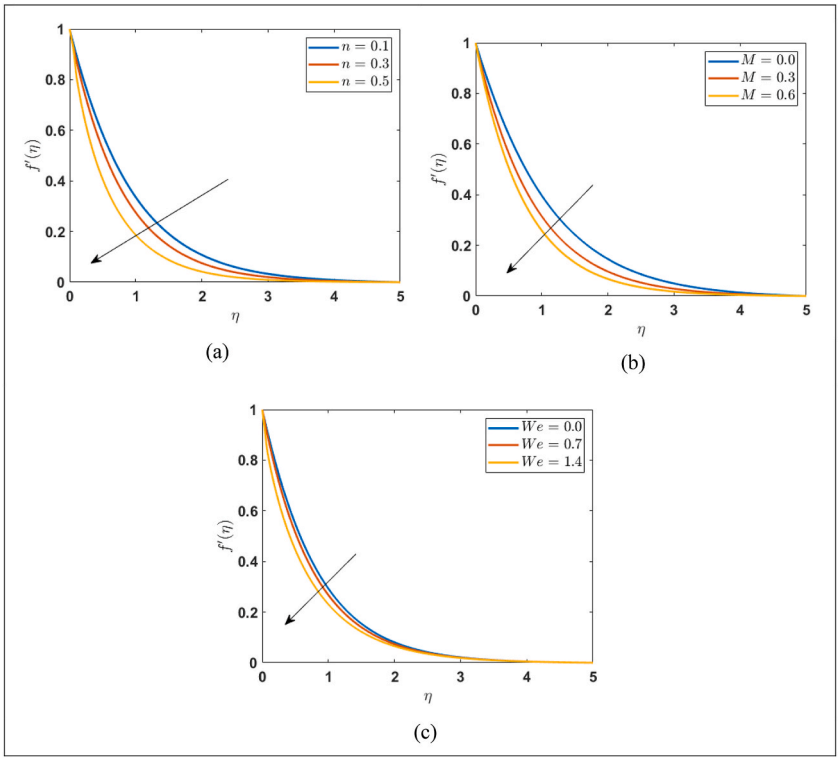

Fig. 2. Profile of $f^{'}(\eta)$ for various values of 2(a) n 2(b) M 2(c) We.

$$\eta = \frac{1}{x^{\frac{1}{3}}}\sqrt{\frac{B}{\nu}}y, g = \frac{C - C_\infty}{C_w - C_\infty}, \theta = \frac{T - T_\infty}{T_w - T_\infty} \tag{6}$$

Using Eq. (6) in equations (1)–(4), we get the following non-dimensional set of ODEs (7–9)

$$\left((1-n) + nWef^{''}\right)f^{'''} - \frac{f^{'2}}{3} - Mf^{'} + \frac{2}{3}ff^{''} = 0 \tag{7}$$

$$\theta^{''} + \frac{2}{3}Pr f\theta^{'} + \frac{Nc}{Le}g^{'}\theta^{'} + \frac{Nc}{Le \times Nbt}\theta^{'2} = 0 \tag{8}$$

$$g^{''} + \frac{2}{3}Scfg^{'} + \frac{1}{Nbt}\theta^{''} = 0 \tag{9}$$

After employing Eq. (6) in Eq (5), the boundary conditions reduces to Eq (10), which is given below.

$$f(0) = 0, f^{'}(0) = 1, f^{'}(\infty) \to 0,$$

$$\theta(0) = 1, \theta(\infty) = 0, g(0) = 1, g(\infty) = 0 \tag{10}$$

where,

$M = \frac{\sigma B_0^2}{B\rho_f}x^{\frac{2}{3}}$ denotes the magnetic parameter, $We = \sqrt{\frac{2B^3}{\nu}}$ is used for Weissenberg number.

$Pr = \frac{\nu}{\alpha}$ represents Prandtl number, $Sc = \frac{\nu}{D_B}$ represents Schmidt Number, $Le = \frac{\alpha}{D_B}$ shows the Lewis number, $Nbt = \frac{D_B\, T_\infty (C_w - C_\infty)}{D_T (T_w - T_\infty)}$ represents diffusivity parameter and $Nc = \frac{\rho_p c_p}{\rho c}(C_w - C_\infty)$ is heat capacity ratio.

The skin friction coefficient (c_f), Nusselt number (N_{u_x}) and Sherwood number (Sh_x) are defined in Equations 11–13 and given below:

$$c_f = \frac{\tau_w}{\rho U_w^2} \tag{11}$$

$$N_{u_x} = \frac{xq_w}{(T_w - T_\infty)} \tag{12}$$

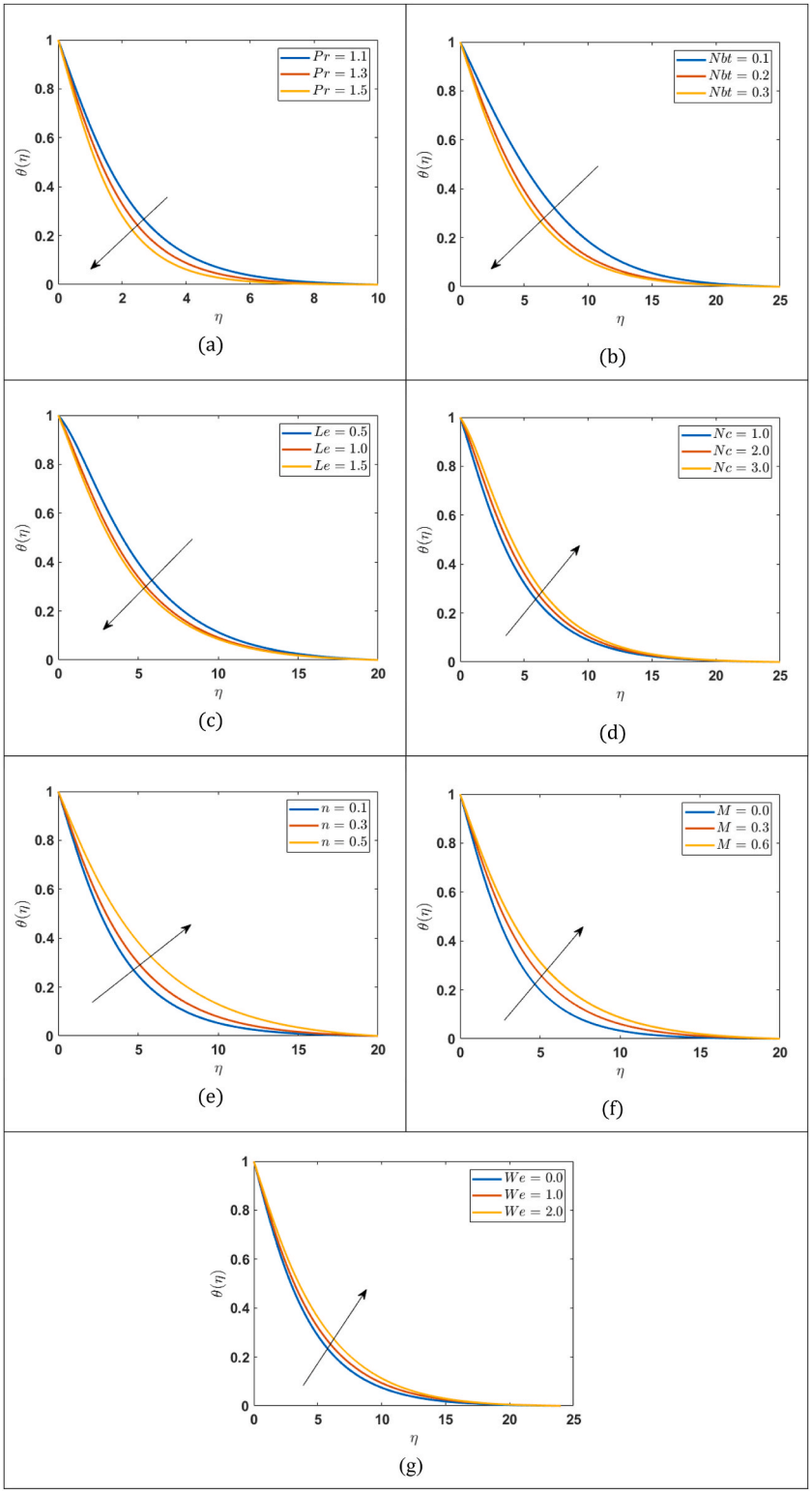

Fig. 3. Profile of $\theta(\eta)$ for different values of 3(a) *Pr* 3(b) *Nbt* 3(c) *Le* 3(d) *Nc* 3(e) *n* 3(f) *M* 3(g) *We*.

$$Sh_x = \frac{xq_s}{(T_w - T_\infty)} \tag{13}$$

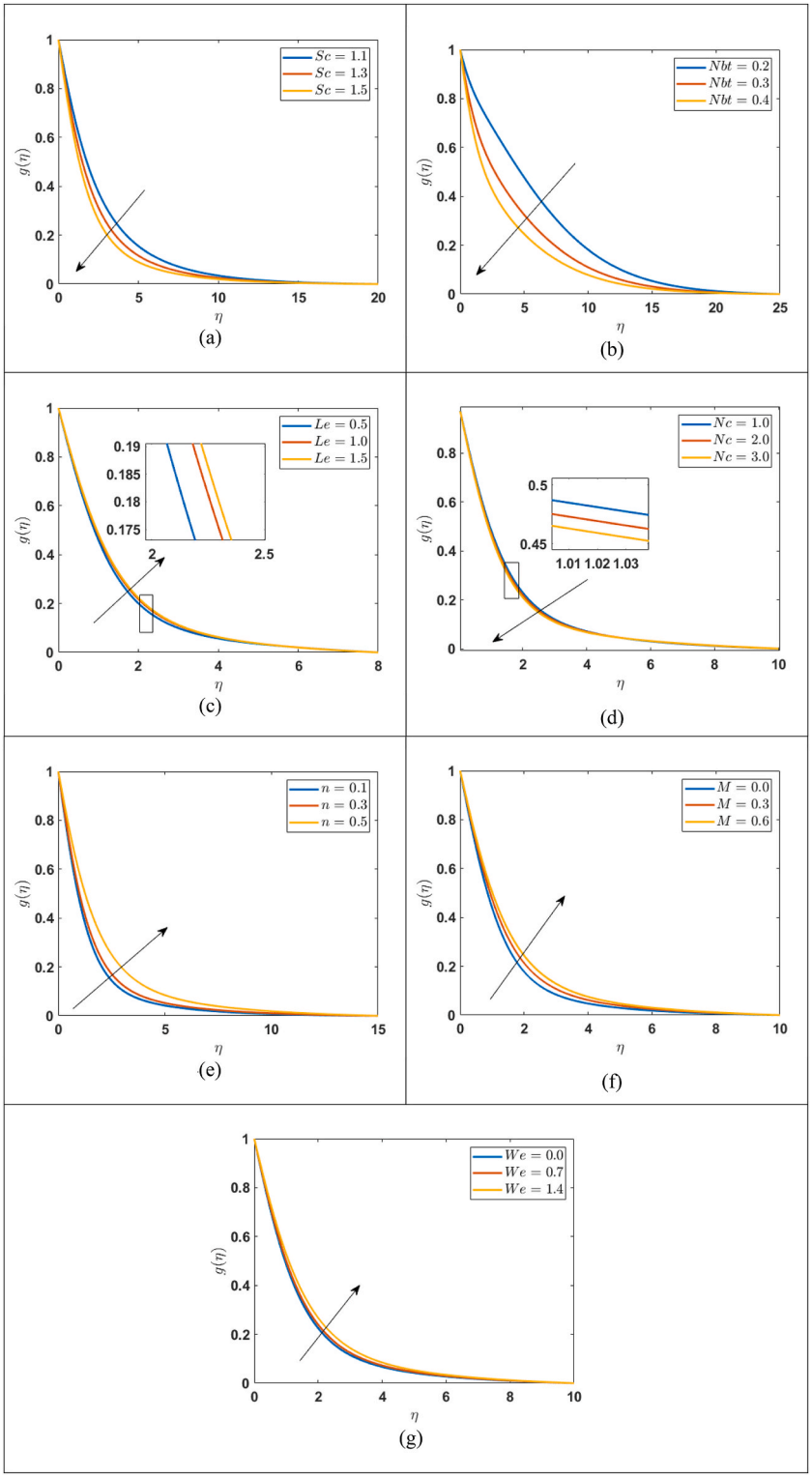

Fig. 4. Profile of $g(\eta)$ for various values of 4(a) *Sc* 4(b) *Nbt* 4(c) *Le* 4(d) *Nc* 4(e) *n* 4(f) *M* 4(g) *We*.

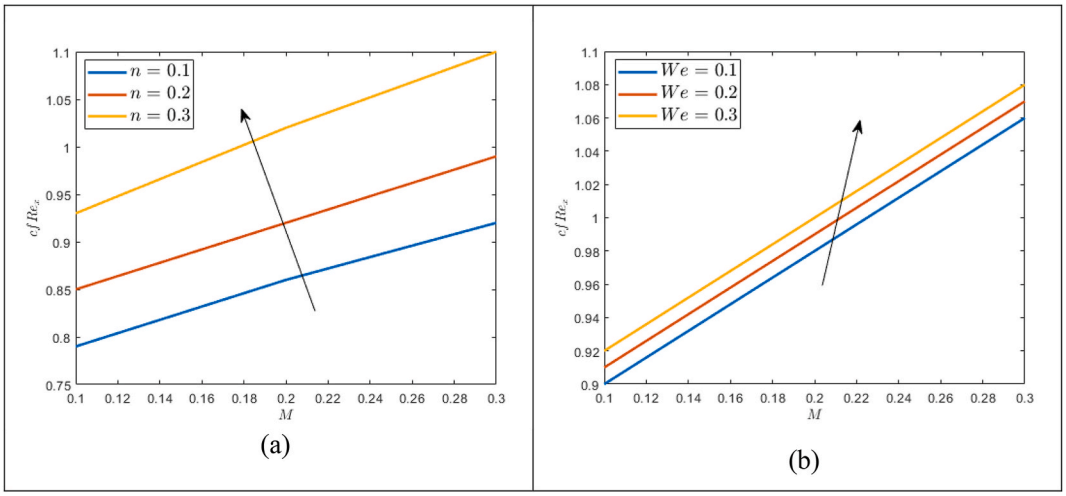

Fig. 5. Behavior of $c_f Re_x$ against M for various values of (a) n (b) We.

where

$\tau_w = (1-n)\frac{\partial u}{\partial y} + \frac{n\Gamma}{\sqrt{2}}\left(\frac{\partial u}{\partial y}\right)^2_{y=0}$,

$q_n = -\left(\frac{\partial T}{\partial y}\right)_{y=0}$,.

$q_s = -\left(\frac{\partial C}{\partial y}\right)_{y=0}$,.

Dimensionless forms of c_f , N_{u_x} and Sh_x are given in Equations 14–16.

$$Re_x c_f = \left((1-n) + \frac{n}{2} We f''(0)\right) f''(0), \tag{14}$$

$$\frac{N_{u_x}}{Re_x} = -\theta'(0) \tag{15}$$

$$\frac{Sh_x}{Re_x} = -g'(0) \tag{16}$$

3. Results and discussion

This paper examines the magnetized Flow of Hyperbolic Tangent Nanofluid across a Non-Linear Stretching Sheet numerically**.** The governing equations are nonlinear PDEs, which are changed into ODEs by adopting suitable similarity transformations. MATLAB solver bvp4c is used to solve system of ODEs. The impacts of *n*, *M* and *We* on the skin friction coefficient $Re_x c_f$ are illustrated in Table 1. The skin friction grows as the *n* and *M* is increased and decreases for Wassenberg number *We*. The impact of *n*, *We*, *M*, *Pr*, *Le*, *Nc*, *Nbt*, and *Sc* on $-\theta'(0)$ and $-g'(0)$ is shown in Table 2. The numerical results presented in Table 2 reveals that the Nusselt number $-\theta'(0)$ increase for *Pr*, *Le*, *Nbt*, and *Sc* and decreases for *n*, *We*, *M*, and *Nc*. The values presented in Table 2 also show that the Sherwood number $-g'(0)$ increase for *Nc*, *Nbt*, and *Sc* and decreases for *n*, *We*, *M*, *Pr*, and *Le*. In Table 3, we presented the numerical results for the Nusselt number $-\theta'(0)$ for different values of *We* and *Pr*. The results presented in Table 3 show that our findings are in good agreement with the results obtained by Kamran et al. [37].

Fig. 2a–c show the influence of *n*, *We*, and *M* on $f'(\eta)$. Fig. 2(a) shows that *n* illustrates the thickening behavior of the fluid. In under discussed fluids, *n* is directly related to the fluid resistance rate. As a result, resistance to the fluid increases as n increases $f'(\eta)$ decreases. Weissenberg number *We* is the ratio of relaxation time to fluid flow time scale. It is shown in Fig. 2(b), when *We* increases, further time is needed for the fluid flow, therefore $f'(\eta)$ decreases. Fig. 2(c) display the effect of Magnetic parameter *M* on $f'(\eta)$. As value of *M* increases, then Lorentz force decreases the fluid velocity, which slows down the motion of fluid.

Fig. 3a–g display the impact of *Pr*, *Nbt*, *Le*, *Nc*, *n*, *We*, and *M* on $\theta(\eta)$. As we Prandtl number *Pr* grows, the $\theta(\eta)$ decreases as shown in Fig. 3(a). As the Prandtl number *Pr* increases, the kinematic viscosity becomes stronger than the thermal diffusivity, resulting in greater resistance to fluid flow. The effect of diffusivity ratio *Nbt* on $\theta(\eta)$ is shown in Fig. 3(b). So, by increasing *Nbt*, $\theta(\eta)$ decreases and thermal boundary layer thickness decreases. Fig. 3(c) display the influence of the Lewis Number *Le* on $\theta(\eta)$. it is the ratio of thermal diffusion to Brownian diffusion. Therefore, as *Le* increases, the $\theta(\eta)$ decreases. The influence of heat capacity ratio *Nc* on $\theta(\eta)$ is shown in Fig. 3(d). Physically, in *Nc*, particles exert a force on other particles, causing them to migrate from hotter place to cooler place. Hence, increasing the value of the *Nc* means applying more force to the other particles, causing more fluid to migrate. As, there is an increase in $\theta(\eta)$ and

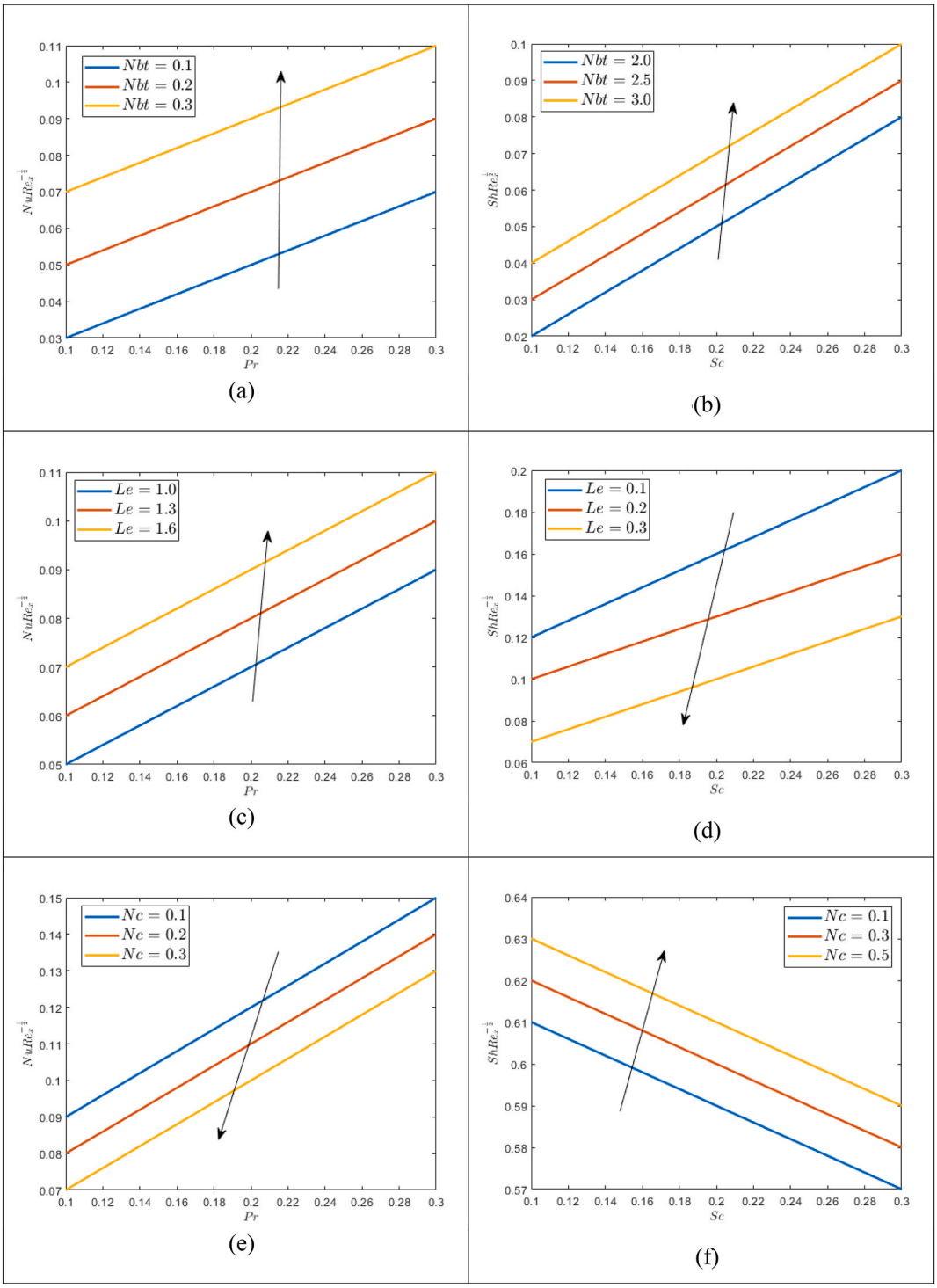

Fig. 6. Influence of *Pr* and *Sc* on $N_u Re_x^{-\frac{1}{2}}$ and $S_h Re_x^{-\frac{1}{2}}$.

$g(\eta)$ as shown in Fig. 3(d). while a reduction is found in the concentration profile $g(\eta)$ as illustrated in Fig. 4(d). The temperature profile $\theta(\eta)$ increase by increasing *n*, *We*, and *M* as illustrated in Fig. 3e–g.

The impact of *Sc* on $g(\eta)$ is illustrated in Fig. 4(a). The $g(\eta)$ is reduced by increasing the *Sc*. Because Sc is the ratio of momentum diffusivity to Brownian diffusivity, increasing Sc induces a decrease in Brownian diffusivity, resulting in a weaker concentration profile. The concentration profile $g(\eta)$ increase by increasing *Le*, *n*, *We*, and *M* as illustrated in Fig. 4e–g while decreases by increasing

Nbt, and *Nc* as shown in Fig. 4b and d. The impact of M on $Re_x c_f$ is observed in Fig. 5. In Fig. 5(a), it has been observed that $Re_x c_f$ increases for increasing values of n and a similar trend has been observed for increasing values of in Fig. 5(b). The graphs of heat transfer rate $N_u Re_x^{-\frac{1}{2}}$ versus growing values of *Pr* and Sherwood number $S_h Re_x^{-\frac{1}{2}}$ against *Sc* have been analyzed in Fig. (6). In Fig. 6(a), it is observed that heat transfer rate $N_u Re_x^{-\frac{1}{2}}$ increases with the increasing values of N_{bt} and a similar trend has been observed for Sherwood number $S_h Re_x^{-\frac{1}{2}}$ in Fig. 6(b). In Fig. (6c-6d), we observed that heat transfer rate increases with the increasing values of *Le*, while the Sherwood number decreases with the increasing values of *Le*. The graphs on Fig. (6e -6f) show that the heat transfer rate $N_u Re_x^{-\frac{1}{2}}$ decreases whereas Sherwood number increases for increasing values of N_c.

4. Conclusion

This article examines the hyperbolic tangent flow in MHD over a non-linear stretching sheet numerically. The following is a list of this study's key characteristics.

- The $f'(\eta)$ and $f''(\eta)$ show reduction for *We*.
- The $\theta(\eta)$ and $g(\eta)$ increase by increasing *We*.
- When *M* is increased, the $f'(\eta)$ decreases while the $\theta(\eta)$ and $g(\eta)$ increases.
- $\theta(\eta)$ decreases on growing *Pr*, *Le*, and *Nbt*.

Author contribution statement

Iftikhar Ahmed: Conceived and designed the experiments; Analyzed and interpreted the data; Wrote the paper.
Metib Alghamdi: Performed the experiments; Wrote the paper.
Muhammad Amjad: Performed the experiments; Contributed reagents, materials, analysis tools or data; Wrote the paper.
Faisal Aziz: Analyzed and interpreted the data.
Tanvir Akbar: Analyzed and interpreted the data; Contributed reagents, materials, analysis tools or data; Wrote the paper.
Taseer Muhammad: Performed the experiments; Contributed reagents, materials, analysis tools or data.

Data availability statement

No data was used for the research described in the article.

Declaration of competing interest

The authors declare that they have no known competing financial interests or personal relationships that could have appeared to influence the work reported in this paper.

Acknowledgment

The authors extend their appreciation to the Deanship of Scientific Research at King Khalid University, Abha, Saudi Arabia for funding this work through Large Groups Project under grant number RGP.2/329/44.

References

[1] F. Shahzad, M. Sagheer, S. Hussain, MHD tangent hyperbolic nanofluid with chemical reaction, viscous dissipation and Joule heating effects, AIP Adv. 9 (2019), 25007.
[2] Z. Ullah, G. Zaman, Lie group analysis of magnetohydrodynamic tangent hyperbolic fluid flow towards a stretching sheet with slip conditions, Heliyon 3 (2017), e00443.
[3] N.S. Akbar, S. Nadeem, R.U. Haq, Z.H. Khan, Numerical solutions of magnetohydrodynamic boundary layer flow of tangent hyperbolic fluid towards a stretching sheet, Indian J. Phys. 87 (2013) 1121–1124.
[4] W. Ibrahim, Magnetohydrodynamics (MHD) flow of a tangent hyperbolic fluid with nanoparticles past a stretching sheet with second order slip and convective boundary condition, Results Phys. 7 (2017) 3723–3731.
[5] H.I. Andersson, MHD flow of a viscoelastic fluid past a stretching surface, Acta Mech. 95 (1992) 227–230.
[6] P.K. Kameswaran, S. Shaw, P. Sibanda, P. Murthy, Homogeneous–heterogeneous reactions in a nanofluid flow due to a porous stretching sheet, Int. J. Heat Mass Tran. 57 (2013) 465–472.
[7] A. Chakrabarti, A.S. Gupta, Hydromagnetic flow and heat transfer over a stretching sheet, Q. Appl. Math. 37 (1979) 73–78.
[8] M. Khan, A. Hussain, M.Y. Malik, T. Salahuddin, F. Khan, Boundary layer flow of MHD tangent hyperbolic nanofluid over a stretching sheet: a numerical investigation, Results Phys. 7 (2017) 2837–2844.
[9] M.Y. Malik, T. Salahuddin, A. Hussain, S. Bilal, MHD flow of tangent hyperbolic fluid over a stretching cylinder: using Keller box method, J. Magn. Magn Mater. 395 (2015) 271–276.
[10] C.-W. Zhang, J.-P. Ou, J.-Q. Zhang, Parameter optimization and analysis of a vehicle suspension system controlled by magnetorheological fluid dampers, Struct. Control Heal. Monit. Off. J. Int. Assoc. Struct. Control Monit. Eur. Assoc. Control Struct. 13 (2006) 885–896.
[11] S.M. Mousavi, A.A.R. Darzi, O. ali Akbari, D. Toghraie, A. Marzban, Numerical study of biomagnetic fluid flow in a duct with a constriction affected by a magnetic field, J. Magn. Magn Mater. 473 (2019) 42–50.

[12] R. Sarlak, S. Yousefzadeh, O.A. Akbari, D. Toghraie, S. Sarlak, others, the investigation of simultaneous heat transfer of water/Al2O3 nanofluid in a close enclosure by applying homogeneous magnetic field, Int. J. Mech. Sci. 133 (2017) 674–688.
[13] D. Toghraie, S.M. Alempour, M. Afrand, Experimental determination of viscosity of water based magnetite nanofluid for application in heating and cooling systems, J. Magn. Magn Mater. 417 (2016) 243–248.
[14] P. Barnoon, D. Toghraie, F. Eslami, B. Mehmandoust, Entropy generation analysis of different nanofluid flows in the space between two concentric horizontal pipes in the presence of magnetic field: single-phase and two-phase approaches, Comput. \& Math. with Appl. 77 (2019) 662–692.
[15] F. Wang, M.I. Asjad, S.U. Rehman, B. Ali, S. Hussain, T.N. Gia, T. Muhammad, MHD Williamson nanofluid flow over a slender elastic sheet of irregular thickness in the presence of bioconvection, Nanomaterials 11 (2021) 2297.
[16] M. Amjad, M.N. Khan, K. Ahmed, I. Ahmed, T. Akbar, S.M. Eldin, Magnetohydrodynamics tangent hyperbolic nanofluid flow over an exponentially stretching sheet: numerical investigation, Case Stud. Therm. Eng. (2023), 102900.
[17] Y.-X. Li, M.H. Alshbool, Y.-P. Lv, I. Khan, M.R. Khan, A. Issakhov, Heat and mass transfer in MHD Williamson nanofluid flow over an exponentially porous stretching surface, Case Stud. Therm. Eng. 26 (2021), 100975.
[18] K. Ahmed, T. Akbar, T. Muhammad, M. Alghamdi, Heat transfer characteristics of MHD flow of Williamson nanofluid over an exponential permeable stretching curved surface with variable thermal conductivity, Case Stud. Therm. Eng. 28 (2021), 101544.
[19] M. Amjad, K. Ahmed, T. Akbar, T. Muhammad, I. Ahmed, A.S. Alshomrani, Numerical investigation of double diffusion heat flux model in Williamson nanofluid over an exponentially stretching surface with variable thermal conductivity, Case Stud. Therm. Eng. 36 (2022), 102231.
[20] I. Ullah, I. Khan, S. Shafie, MHD natural convection flow of Casson nanofluid over nonlinearly stretching sheet through porous medium with chemical reaction and thermal radiation, Nanoscale Res. Lett. 11 (2016) 1–15.
[21] T. Hayat, S. Qayyum, A. Alsaedi, B. Ahmad, Magnetohydrodynamic (MHD) nonlinear convective flow of Walters-B nanofluid over a nonlinear stretching sheet with variable thickness, Int. J. Heat Mass Transf. 110 (2017) 506–514.
[22] P.K. Kameswaran, P. Sibanda, M.K. Partha, P. Murthy, Thermophoretic and nonlinear convection in non-Darcy porous medium, J. Heat Transfer. 136 (2014).
[23] R. Cortell, Viscous flow and heat transfer over a nonlinearly stretching sheet, Appl. Math. Comput. 184 (2007) 864–873.
[24] X.-Q. Wang, A.S. Mujumdar, Heat transfer characteristics of nanofluids: a review, Int. J. Therm. Sci. 46 (2007) 1–19.
[25] S.U.S. Choi, J.A. Eastman, Enhancing Thermal Conductivity of Fluids with Nanoparticles, 1995.
[26] P.P. Gharami, S. Reza-E-Rabbi, S.M. Arifuzzaman, M.S. Khan, T. Sarkar, S.F. Ahmmed, MHD effect on unsteady flow of tangent hyperbolic nano-fluid past a moving cylinder with chemical reaction, SN Appl. Sci. 2 (2020) 1–16.
[27] K.-E. Aslani, I.E. Sarris, Effect of micromagnetorotation on magnetohydrodynamic Poiseuille micropolar flow: analytical solutions and stability analysis, J. Fluid Mech. 920 (2021) A25.
[28] A.A. Gkountas, L.T. Benos, G.N. Sofiadis, I.E. Sarris, A printed-circuit heat exchanger consideration by exploiting an Al2O3-water nanofluid: effect of the nanoparticles interfacial layer on heat transfer, Therm. Sci. Eng. Prog. 22 (2021), 100818.
[29] M. Amjad, I. Ahmed, K. Ahmed, M.S. Alqarni, T. Akbar, T. Muhammad, Numerical solution of magnetized williamson nanofluid flow over an exponentially stretching permeable surface with temperature dependent viscosity and thermal conductivity, Nanomaterials 12 (2022) 3661.
[30] A. Ahmadian, M. Bilal, M.A. Khan, M.I. Asjad, The non-Newtonian maxwell nanofluid flow between two parallel rotating disks under the effects of magnetic field, Sci. Rep. 10 (2020), 17088.
[31] Y.-M. Chu, R. Ali, M.I. Asjad, A. Ahmadian, N. Senu, Heat transfer flow of Maxwell hybrid nanofluids due to pressure gradient into rectangular region, Sci. Rep. 10 (2020), 16643.
[32] K. Ahmed, T. Akbar, T. Muhammad, M. Alghamdi, Heat transfer characteristics of MHD flow of Williamson nanofluid over an exponential permeable stretching curved surface with variable thermal conductivity, Case Stud. Therm. Eng. 28 (2021), 101544.
[33] B. Ali, R.A. Naqvi, Y. Nie, S.A. Khan, M.T. Sadiq, A.U. Rehman, S. Abdal, Variable viscosity effects on unsteady MHD an axisymmetric nanofluid flow over a stretching surface with thermo-diffusion: fem approach, Symmetry (Basel). 12 (2020) 234.
[34] A. Farooq, A. Salahuddin, M. Razzaq, S. Hussain, A. Mushtaq, Computational Analysis of Unsteady and Steady Magnetohydrodynamic Radiating Nano Fluid Flows Past a Slippery Stretching Sheet Immersed in a Permeable Medium, 2020.
[35] S. Abdal, B. Ali, S. Younas, L. Ali, A. Mariam, Thermo-diffusion and multislip effects on MHD mixed convection unsteady flow of micropolar nanofluid over a shrinking/stretching sheet with radiation in the presence of heat source, Symmetry (Basel). 12 (2019) 49.
[36] L. Yang, J. Huang, M. Mao, W. Ji, Numerical assessment of Ag-water nano-fluid flow in two new microchannel heatsinks: thermal performance and thermodynamic considerations, Int. Commun. Heat Mass Transf. 110 (2020), 104415.
[37] K. Anantha Kumar, V. Sugunamma, N. Sandeep, Influence of viscous dissipation on MHD flow of micropolar fluid over a slendering stretching surface with modified heat flux model, J. Therm. Anal. Calorim. 139 (2020) 3661–3674.
[38] R. Ali, M.R. Khan, A. Abidi, S. Rasheed, A.M. Galal, Application of PEST and PEHF in magneto-Williamson nanofluid depending on the suction/injection, Case Stud. Therm. Eng. 27 (2021), 101329.
[39] K. Ahmed, T. Akbar, Numerical investigation of magnetohydrodynamics Williamson nanofluid flow over an exponentially stretching surface, Adv. Mech. Eng. 13 (2021), 16878140211019876.
[40] N.S. Akbar, D. Tripathi, Z.H. Khan, Numerical investigation of Cattanneo-Christov heat flux in CNT suspended nanofluid flow over a stretching porous surface with suction and injection, Discret. \& Contin. Dyn. Syst. 11 (2018) 583.